

INCIDENT-ANGLE DEPENDENCE OF ELECTROMAGNETIC TRANSMISSION THROUGH A PLASMONIC SCREEN WITH A NANO-APERTURE

Désiré MIESSEIN^{1,2*}, Norman J. M. HORING¹, Harry LENZING¹, Godfrey GUMBS³

¹ STEVENS INSTITUT OF TECHNIQUE, Department of Physics and Engineering Physics, Hoboken, New Jersey 07030, USA (*dmiessei@stevens.edu);

² FORDHAM UNIVERSITY, Department of Physics and Engineering Physics, Bronx, New York 10458, USA;

³ HUNTER COLLEGE OF THE CITY UNIVERSITY OF NEW YORK, Department of Physics and Astronomy, New York, New York 10065, USA

Abstract:

The dependence of electromagnetic transmission through a subwavelength nano-hole in a plasmonic layer on angle of incidence is examined here for both p- and s-polarizations. Calculations are carried out for a sampling of incident angles, and the dyadic Greens function method employed includes the interference between transmission emanating from the nano-hole and transmission directly through the plasmonic screen. The integral equation formulation employed for the Greens function obviates the need for a separate imposition of boundary conditions (and no appeal to ideal metallic boundary conditions is involved). Interference fringes cluster about the aperture and flatten to uniform transmission far from it. Furthermore, as the incident angle increases, the axis of the relatively large central transmission maximum through the nano-hole follows it, accompanied by a spatial compression of interference fringe maxima forward of the large central transmission maximum, and a spatial thinning of the fringe maxima behind it. For p-polarization, the transmission results show a strong increase as the incident angle θ_0 increases, mainly in the dominant E_z component (notwithstanding a concomitant decrease of the E_x component as θ_0 increases). We also find that in the case of s-polarization of the incident electromagnetic wave, the transmission decreases as θ_0 increases. These results, for both p- and s-polarizations, are consistent with earlier results for perfect metal boundary conditions, although such ideal boundary conditions are not invoked here as we have treated the problem of a nano-hole in a semiconductor layer and have determined its electromagnetic transmission including the role of its two dimensional plasma.

Keywords: Dyadic Green's function, Incident-Angle Dependence, Electromagnetic Wave Transmission, Nano-hole, Thin Plasmonic Semiconductor Layer.

1. Introduction

In a recent study of electromagnetic wave transmission through a nano-hole in a thin, smooth, planar plasmonic semiconductor layer Fig.2.1, we examined subwavelength transmission in detail for normal incidence of the wave train [1-5]. Our dyadic Green's function integral equation formulation eliminated the need for separate, explicit treatment of the boundary conditions used in earlier works [6,7]. Other important works [8-10] using dyadic Green's functions [11-14] and variational principles assumed the layer to be a perfect, ideal metallic

conductor, whereas our present interest considers the layer to be a thin, smooth, planar plasmonic semiconductor.

A plethora of recent theoretical and experimental electromagnetic research began with the report of extraordinary optical transmission by Ebbeson, et al. [15]. Much of this work is reviewed by Garcia-Vidal, et al.: "Light Passing Through subwavelength Apertures"[16], and the years since this 2010 review have seen further developments, both experimental and theoretical. A variety of electromagnetic studies have treated apertures that are mostly subwavelength (and some not so small)

Désiré Miessein, Norman J. M. Horing, Harry Lenzing, Godfrey Gumbs

Incident-Angle Dependence of EM Transmission Through a plasmonic Screen with a Nano-Aperture

embedded in layers of varying thickness; some studies addressed perfect, ideal metallic layers, others treated real semiconductor layers involving plasmas. Most treated normal incidence, a few addressed oblique incidence. A representative list of pertinent articles is presented in chronological order in the References [17-39].

Our earlier work [1] involved the analytic determination of the dyadic electromagnetic Green's function for the system in closed form, facilitating relatively simple calculation of the transmitted radiation through both the hole as well as through the layer itself for normal incidence. Employment of the dyadic Green's function in an integral equation formulation automatically embedded the roles of the electromagnetic boundary conditions and the 2D plasmon in the layer (which is "smeared" due to its lateral wavenumber dependence), obviating the need for separate treatment. In the present paper, we employ the same method to analyze subwavelength Electromagnetic transmission through such a system for *non*-normal incidence [40] of the electromagnetic wave train on the nano-hole. In Section 2, we review the appropriate dyadic Green's function for the perforated plasmonic screen with a subwavelength aperture and its application to electromagnetic transmission in the construction of the system's inverse dielectric tensor, with emphasis on non-normal incidence. The calculated results for various angles of incidence are exhibited in the figures of Section 3, and a summary is presented in Section 4.

2. Dyadic Green's Function and Inverse Dielectric Tensor

Figure 2.1 illustrates a two dimensional plasmonic layer (thickness d , embedded at $z=0$ in a three dimensional bulk medium) with a nano-hole of radius R , area A at the origin of the $(x-y)$ plane. The dyadic Green's function for such a thin perforated plasmonic screen with a nano-hole was determined as

$$(\beta = \gamma A = \frac{4i\pi\omega}{c^2} \sigma_{fs}^{(2D)}(\omega)A; A \text{ is area of the nano-hole):}$$

$$\hat{G}(\vec{r}_{//}, 0; z, 0; \omega) = \hat{G}_{fs}(\vec{r}_{//}, 0; z, 0; \omega) \times \left[\hat{I} + \beta \hat{G}_{fs}(0, 0; 0, 0; \omega) \right]^{-1} \quad (1)$$

Here, \hat{G}_{fs} is the dyadic Green's function for the thin plasmonic layer in the absence of the subwavelength aperture, and its elements are

given by (c is the speed of light; \hat{I} is the unit dyadic; ω is angular frequency)

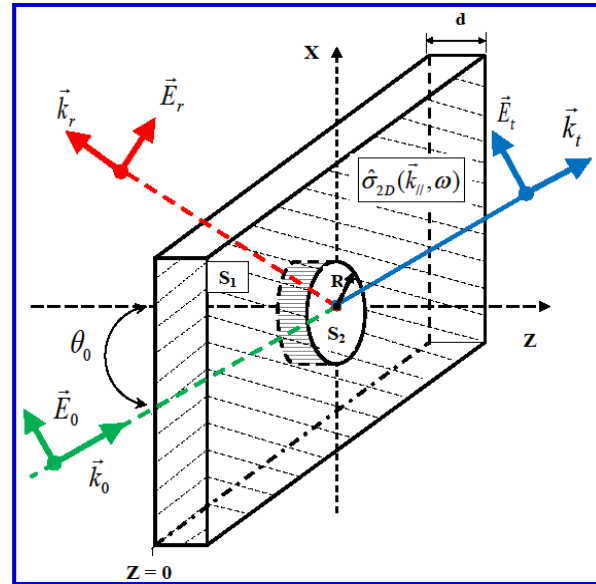


Fig.2.1. Schematic of a two dimensional plasmonic layer (thickness d , embedded at $z = 0$ in a three dimensional bulk medium) with a nano-hole of radius R , area A at the origin of the $(x-y)$ plane, shown with incident, reflected and transmitted wave vectors $(\vec{k}_0, \vec{k}_r, \vec{k}_t)$ for waves $(\vec{E}_0(x, y, z; t), \vec{E}_r(x, y, z; t), \vec{E}_t(x, y, z; t))$. The angle of incidence is θ_0 in the $x-z$ plane ($k_{0y} \equiv 0$).

$$\hat{G}_{fs}(k_x, k_y = 0; z, 0; \omega) =$$

$$\begin{bmatrix} \hat{G}_{fs}^{xx}(k_x, k_y = 0; z, 0; \omega) & 0 & \hat{G}_{fs}^{xz}(k_x, k_y = 0; z, 0; \omega) \\ 0 & \hat{G}_{fs}^{yy}(k_x, k_y = 0; z, 0; \omega) & 0 \\ \hat{G}_{fs}^{zx}(k_x, k_y = 0; z, 0; \omega) & 0 & \hat{G}_{fs}^{zz}(k_x, k_y = 0; z, 0; \omega) \end{bmatrix} \quad (2)$$

where $\vec{k}_{//} = (k_x, k_y)$ is wavevector parallel to the plasmonic screen, $\sigma_{fs}^{(2D)}$ is the conductivity of the full plasmonic sheet and the matrix elements of \hat{G}_{fs} are given by

$$G_{fs}^{xx}(k_x, k_y = 0; z, 0; \omega) = -\frac{e^{ik_z|z|}}{2ik_z} \left[\frac{1}{D_1} \left\{ 1 - \frac{k_x^2}{q_\omega^2} \right\} \right], \quad (3)$$

$$G_{fs}^{yy}(k_x, k_y = 0; z, 0; \omega) = -\frac{e^{ik_z|z|}}{2ik_z} \left[\frac{1}{D_3} \right], \quad (4)$$

$$G_{fs}^{zz}(k_x, k_y = 0; z, 0; \omega) = -\frac{e^{ik_z|z|}}{2ik_z} \left[\frac{1}{D_2} \left\{ 1 - \frac{k_z^2 - 2ik_z\delta(z)}{q_\omega^2} \right\} \right], \quad (5)$$

$$G_{fs}^{xy}(k_x, k_y = 0; z, 0; \omega) = 0, \quad (6)$$

Désiré Miessein, Norman J. M. Horing, Harry Lenzing, Godfrey Gumbs

Incident-Angle Dependence of EM Transmission Through a plasmonic Screen with a Nano-Aperture

$$G_{fs}^{xz}(k_x, k_y = 0; z, 0; \omega) = + \frac{e^{ik_z|z|}}{2ik_z} \left[\frac{1}{\bar{D}_2} \left\{ \left(\frac{k_x k_z \text{sgn}(z)}{q_\omega^2} \right) \right\} \right], \quad (7)$$

$$G_{fs}^{yz}(k_x, k_y = 0; z, 0; \omega) = 0, \quad (8)$$

$$G_{fs}^{yx}(k_x, k_y = 0; z, 0; \omega) = 0, \quad (9)$$

$$G_{fs}^{zx}(k_x, k_y = 0; z, 0; \omega) = + \frac{e^{ik_z|z|}}{2ik_z} \left[\frac{1}{\bar{D}_1} \left\{ \left(\frac{k_z k_x \text{sgn}(z)}{q_\omega^2} \right) \right\} \right], \quad (10)$$

$$G_{fs}^{zy}(k_x, k_y = 0; z, 0; \omega) = 0, \quad (11)$$

and

$$\left(\gamma = \frac{4\pi i \omega}{c^2} \sigma_{fs}^{(2D)}(\vec{k}_\parallel; \omega); \sigma_{fs}^{(2D)}(\vec{k}_\parallel; \omega) = \frac{i\omega}{4\pi} [\epsilon_b^{(3D)} - \epsilon(\omega)] d \right)$$

$$\bar{D}_1 = \left[1 + \left(\frac{\gamma}{2ik_z} \right) \left(1 - \frac{k_x^2}{q_\omega^2} \right) \right], \quad (12)$$

$$\bar{D}_2 = \left[1 + \left(\frac{\gamma}{2ik_z} \right) \left(1 - \frac{a_0^2}{q_\omega^2} \right) \right], \quad (13)$$

$$\bar{D}_3 = \left[1 + \left(\frac{\gamma}{2ik_z} \right) \right], \quad (14)$$

with $a_0^2 = k_z^2 - \frac{2ik_z}{d}$

While the dyadic Green's function above determines the electromagnetic response to a current source, it does not, by itself, describe the response to an incident electromagnetic wave field. For that, it is necessary to construct the inverse dielectric tensor of the system which provides the relation between the actual field $\vec{E}(\vec{r}; t)$ and the impressed (incident) field $\vec{E}_0(\vec{r}; t)$.

Considering that $\hat{G}(\vec{r}_\parallel, \vec{r}'_\parallel; z, z'; \omega)$ described above already incorporates the role of induced current, it provides the system's response to an externally impressed current \vec{J}_{ext} alone as

$$\vec{E}(\vec{r}_\parallel, z; \omega) = \frac{4\pi i \omega}{c^2} \int d^2 \vec{r}'_\parallel \int dz' \hat{G}(\vec{r}_\parallel, \vec{r}'_\parallel; z, z'; \omega) \vec{J}_{ext}(\vec{r}'_\parallel, z'; \omega) \quad (15)$$

or

$$\vec{E} = \frac{4\pi i \omega}{c^2} \hat{G} \vec{J}_{ext}, \quad (16)$$

in spatial matrix notation. Bearing in mind that $(\hat{\sigma}_{fs}^{(2D)}, \hat{\sigma}_{hole}^{(2D)})$ are the conductivities of the full 2D screen and the excluded hole, respectively; see Eqns.26, 27 below)

$$\hat{G}^{-1} = \hat{G}_{3D}^{-1} - \frac{4\pi i \omega}{c^2} \hat{\Sigma}_{2D} \quad (17)$$

where

$$\hat{\Sigma}_{2D} = \hat{\sigma}_{fs}^{(2D)} - \hat{\sigma}_{hole}^{(2D)} \quad (18)$$

and that the incident field \vec{E}_0 is related to its distant current source \vec{J}_{ext} by

$$\vec{E}_0 = \frac{4\pi i \omega}{c^2} \hat{G}_{3D} \vec{J}_{ext} \quad (19)$$

or

$$\vec{J}_{ext} = \left[\frac{4\pi i \omega}{c^2} \hat{G}_{3D} \right]^{-1} \vec{E}_0, \quad (20)$$

we have

$$\begin{aligned} \vec{E} &= \hat{G} \hat{G}_{3D}^{-1} \vec{E}_0 \\ &= \hat{G} \left[\hat{G}^{-1} + \frac{4\pi i \omega}{c^2} \hat{\Sigma}_{2D} \right] \vec{E}_0 \\ &= \left[\hat{I} + \frac{4\pi i \omega}{c^2} \hat{G} \hat{\Sigma}_{2D} \right] \vec{E}_0. \end{aligned} \quad (21)$$

Obviously, this introduces the inverse dielectric dyadic/tensor \hat{K} as

$$\hat{K} = \left[\hat{I} + \frac{4\pi i \omega}{c^2} \hat{G} \hat{\Sigma}_{2D} \right], \quad (22)$$

in complete analogy to the results[8], [9] of references [1] and [2].

Thus, we have the actual \vec{E} -field as

$$\vec{E}(\vec{r}_\parallel, z; \omega) = \vec{E}_0(\vec{r}_\parallel, z; \omega) + \vec{E}_1(\vec{r}_\parallel, z; \omega) + \vec{E}_2(\vec{r}_\parallel, z; \omega), \quad (23)$$

where the electric field contributions \vec{E}_1 and \vec{E}_2 are defined by

$$\begin{aligned} \vec{E}_1(\vec{r}_\parallel, z; \omega) &= \frac{4\pi i \omega}{c^2} \int d^2 \vec{r}'_\parallel \int d^2 \vec{r}''_\parallel \int dz' \int dz'' \\ &\times \hat{G}(\vec{r}_\parallel, \vec{r}'_\parallel; z, z'; \omega) \hat{\sigma}_{fs}^{(2D)}(\vec{r}'_\parallel, \vec{r}''_\parallel; z', z''; \omega) \vec{E}_0(\vec{r}''_\parallel, z''; \omega) \end{aligned} \quad (24)$$

and

$$\begin{aligned} \vec{E}_2(\vec{r}_\parallel, z; \omega) &= \frac{4\pi i \omega}{c^2} \int d^2 \vec{r}'_\parallel \int d^2 \vec{r}''_\parallel \int dz' \int dz'' \\ &\times \hat{G}(\vec{r}_\parallel, \vec{r}'_\parallel; z, z'; \omega) \hat{\sigma}_{hole}^{(2D)}(\vec{r}'_\parallel, \vec{r}''_\parallel; z', z''; \omega) \vec{E}_0(\vec{r}''_\parallel, z''; \omega). \end{aligned} \quad (25)$$

Because the conductivities $\hat{\sigma}_{fs}^{(2D)}$ and $\hat{\sigma}_{hole}^{(2D)}$ are confined to the 2D screen at $z = 0$ (thickness d) they may be written in lateral (\vec{r}_\parallel) - and z - representation as

$$\hat{\sigma}_{fs}^{(2D)}(\vec{r}'_\parallel, \vec{r}''_\parallel; z, z'; \omega) = \hat{I} \hat{\sigma}_{fs}^{(2D)}(\omega) \delta^{(2D)}(\vec{r}'_\parallel - \vec{r}''_\parallel) \delta(z') \delta(z'') \quad (26)$$

and

$$\begin{aligned} \hat{\sigma}_{hole}^{(2D)}(\vec{r}_\parallel, \vec{r}'_\parallel; z, z'; \omega) &\approx \hat{I} \hat{A} \hat{\sigma}_{fs}^{(2D)}(\omega) \delta^{(2D)}(\vec{r}_\parallel) \\ &\times \delta^{(2D)}(\vec{r}_\parallel - \vec{r}'_\parallel) \delta(z) \delta(z') \end{aligned} \quad (27)$$

It should be noted that in the absence of the nano-hole, $\hat{A} \mapsto \hat{O}$, the field contribution $\vec{E}_2(\vec{r}_\parallel, z; \omega)$ vanishes, leaving

$$\begin{aligned} \vec{E}(\vec{r}_\parallel, z; \omega) &= \vec{E}_0(\vec{r}_\parallel, z; \omega) + \vec{E}_1(\vec{r}_\parallel, z; \omega) \\ &= \vec{E}_{fs}(\vec{r}_\parallel, z; \omega), \end{aligned} \quad (28)$$

where $\vec{E} \mapsto \vec{E}_{fs}$ jointly with $\hat{G} \mapsto \hat{G}_{fs}$ are the field and associated Green's function (respectively) for the transmission/reflection of the field \vec{E}_0 impinging on the full, unperforated 2D layer.

Finally, the resulting electric field \vec{E} can be written in position representation as

Désiré Miessein, Norman J. M. Horing, Harry Lenzing, Godfrey Gumbs

Incident-Angle Dependence of EM Transmission Through a plasmonic Screen with a Nano-Aperture

$$\vec{E}(\vec{r}_{//}, z; t) = \vec{E}_0(\vec{r}_{//}, z; t) + \gamma_0 \hat{G}_{fs}(\vec{k}_{0y}; z, 0; \omega_0) \vec{E}_0 e^{i[\vec{k}_{0y} \cdot \vec{r}_{//} - \omega_0 t]} - \beta_0 \hat{G}(\vec{r}_{//}, 0; z, 0; \omega_0) \times \left[\hat{I} + \gamma_0 \hat{G}_{fs}(\vec{k}_{0y}; 0, 0; \omega_0) \right] \vec{E}_0 e^{-i\omega_0 t} \quad (29)$$

(notation: $\hat{G}_{fs}(\vec{k}_{0y}; 0, 0; \omega_0) \equiv \hat{\hat{G}}_{fs}(\vec{k}_{0y}; 0, 0; \omega_0)$ emphasizes that both $z = 0$ and $z' = 0$ with a double overbar; also $\gamma_0 = -\frac{d\omega_{p,3D}^2}{c^2}$ and $\omega_{p,3D} = \sqrt{\frac{4\pi e^2 \rho_{3D}}{m}}$ is the 3D bulk plasma frequency; $\beta_0 = \gamma_0 A$; $\Gamma_0 = -\frac{i\gamma_0}{2}$; \vec{k}_0 and ω_0 are the incident wavevector and frequency, respectively; β_0 and γ_0 are β and γ evaluated at incident frequency $\omega = \omega_0$)

$$\hat{\hat{G}}_{fs}^{xx}(\vec{k}_{0y}; 0, 0; \omega_0) = \frac{-\cos(\theta_0)}{2i[q_{\omega_0} + \Gamma_0 \cos(\theta_0)]} \quad (30)$$

$$\hat{\hat{G}}_{fs}^{yy}(\vec{k}_{0y}; 0, 0; \omega_0) = \frac{-1}{2i[\Gamma_0 + q_{\omega_0} \cos(\theta_0)]} \quad (31)$$

and

$$\hat{\hat{G}}_{fs}^{zz}(\vec{k}_{0y}; 0, 0; \omega_0) = \frac{-1}{2i} \left\{ \frac{q_{\omega_0} \sin^2(\theta_0) + 2i\delta(0)\cos(\theta_0)}{\cos(\theta_0)[q_{\omega_0}^2 + 2i\delta(0)\Gamma_0] + q_{\omega_0}\Gamma_0 \sin^2(\theta_0)} \right\}. \quad (32)$$

(Note that $\hat{\hat{G}}_{fs}(\vec{k}_{0y}; 0, 0; \omega_0)$ was shown to be diagonal in reference [1], see appendices)

3. Incident Angle Dependence of Electromagnetic Wave Transmission Through a 2D Plasmonic Layer a Nano-Hole

The results above are employed here to examine the spatial dependence of the diffracted/transmitted wave arising from an incoming electromagnetic wave at an arbitrary angle of incidence, θ_0 , in the x - z plane of incidence ($k_{0y} \equiv 0$). Detailed computations are carried out for incident angles of 30° , 60° and 80° . The figures below present results (based on calculations using Mathematica) for $|E_x(x, y, z; t)/E_0|^2$, $|E_y(x, y, z; t)/E_0|^2$ and $|E_z(x, y, z; t)/E_0|^2$ for spatial regions defined by $z = 300R$ (intermediate zone) and $z = 1000R$ (far zone), with lateral coordinate

$$r_{//} = \sqrt{x^2 + y^2} \text{ extension in the range } r_{//} = 10^3 R - 2 \times 10^3 R = 5 \times 10^3 - 10^4 \text{ nm for both zones.}$$

The results are exhibited in 2D line graphs and in both 3D and density plots for both p - and s -polarizations of the incident wave. In all computations represented in these figures, we employ the following parameters: $R = 5 \text{ nm}$, $d = 10 \text{ nm}$ and $f_0 = 300 \text{ THz}$; the semiconductor screen is taken to be GaAs with effective mass

$m^* = 0.067 m_0$ (m_0 is the free-electron mass) and density $n_{3D} = 4 \times 10^{21} / \text{cm}^3$ ($\epsilon_b^{(3D)} = 1$ is the dielectric constant of the host medium). In Figures 3.1-3.8, we set $y \equiv 0$ and $r_{//} = x$ varies over the indicated zone range, Figures 3.9a-3.18a exhibit 3D plots of the transmitted component power distributions, while Figures 3.9b-3.18b provide the associated component power density plots, all as functions of both x and y for the fixed z -values indicated above.

p - polarization: Middle-Field, $z = 300R$; $\theta_0 = 30^\circ$

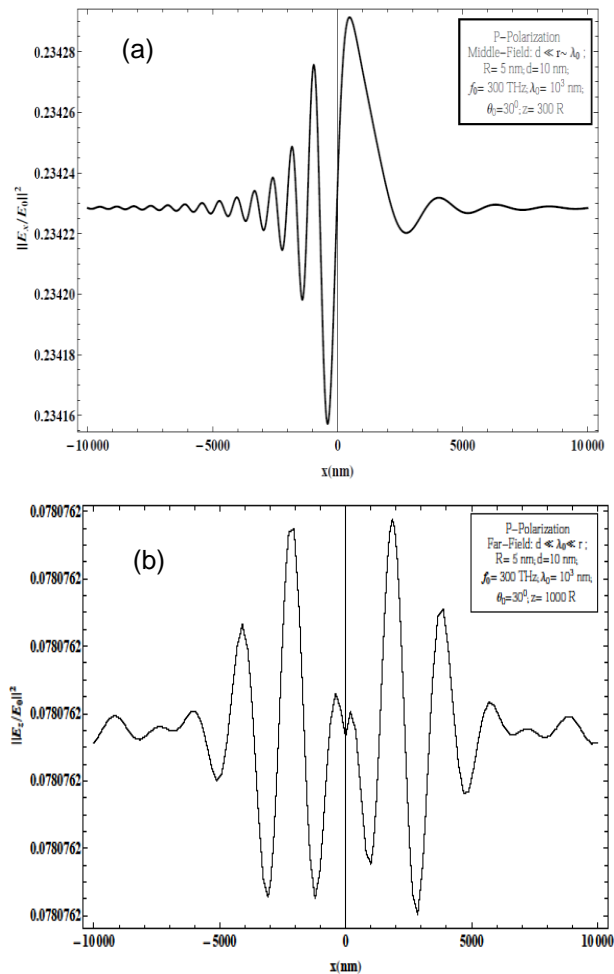


Fig.3.1. p - polarization - Middle-Field, $z = 300R$; $\theta_0 = 30^\circ$: (a) $|E_x(x, y, z; t)/E_0|^2$ and (b) $|E_z(x, y, z; t)/E_0|^2$ produced by a perforated 2D plasmonic layer of GaAs as a function of lateral distance $r_{//} = x(y = 0)$ from the aperture.

Désiré Miessein, Norman J. M. Horing, Harry Lenzing, Godfrey Gumbs

Incident-Angle Dependence of EM Transmission Through a plasmonic Screen with a Nano-Aperture

ρ - polarization: Middle-Field, $z = 300R$; $\theta_0 = 60^\circ$

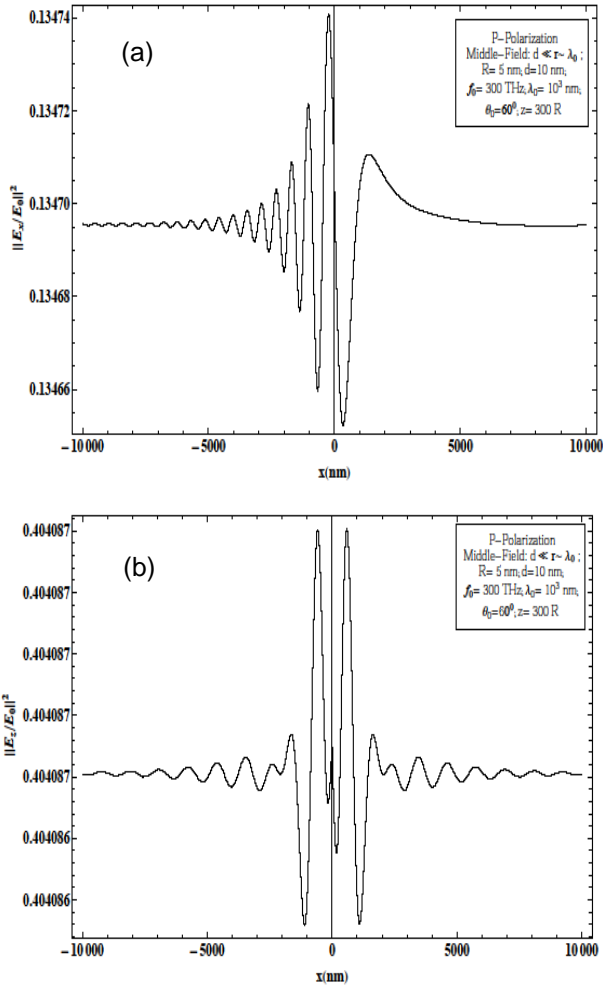


Fig.3.2. ρ - polarization-Middle - Field, $z = 300R$; $\theta_0 = 60^\circ$: (a) $|E_x(x, y, z; t)/E_0|^2$ and (b) $|E_z(x, y, z; t)/E_0|^2$ produced by a perforated 2D plasmonic layer of GaAs as a function of lateral distance $r_{//} = x(y = 0)$ from the aperture.

ρ - polarization: Middle-Field, $z = 300R$; $\theta_0 = 80^\circ$

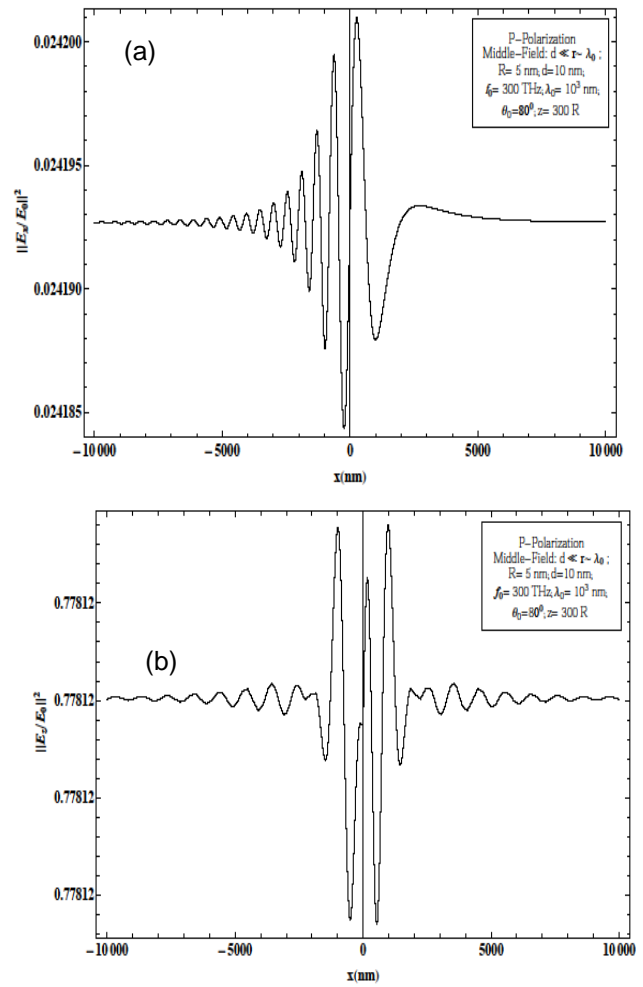


Fig.3.3. ρ - polarization - Middle-Field, $z = 300R$; $\theta_0 = 80^\circ$: (a) $|E_x(x, y, z; t)/E_0|^2$ and (b) $|E_z(x, y, z; t)/E_0|^2$ produced by a perforated 2D plasmonic layer of GaAs as a function of lateral distance $r_{//} = x(y = 0)$ from the aperture.

Désiré Miessein, Norman J. M. Horing, Harry Lenzing, Godfrey Gumbs

Incident-Angle Dependence of EM Transmission Through a plasmonic Screen with a Nano-Aperture

s - polarization: Middle-Field, $z = 300 R$

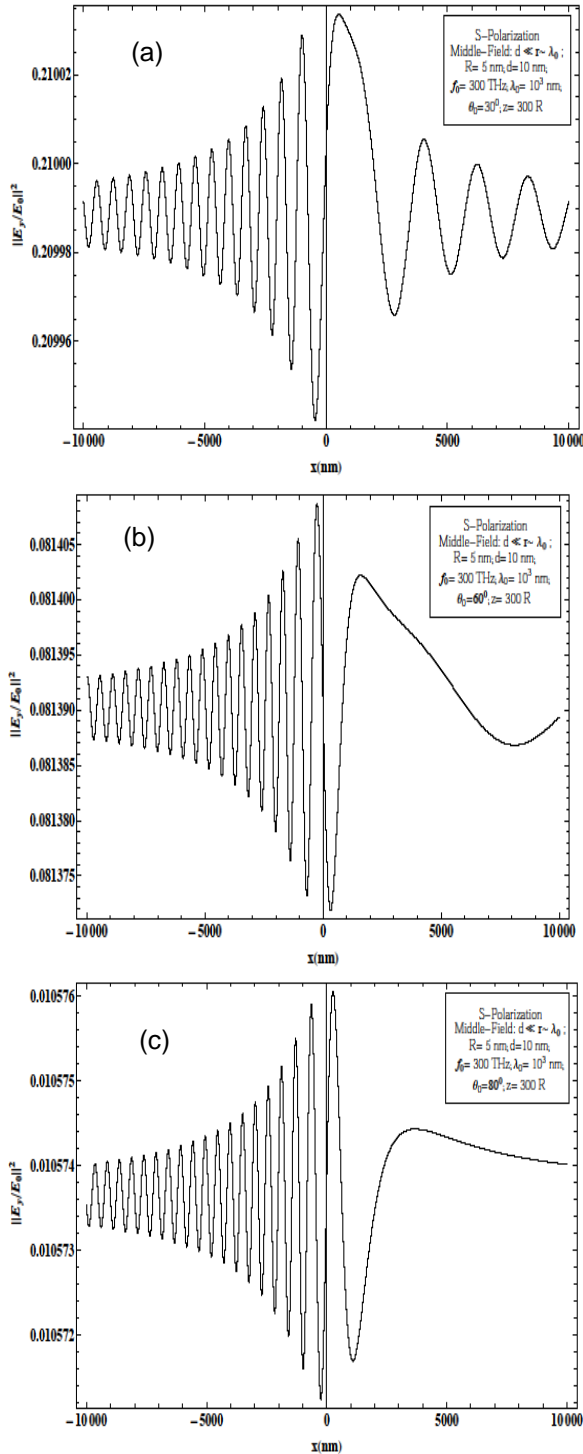


Fig.3.4. s - polarization-Middle - Field, $z = 300 R$; $|E_x(x, y, z; t)/E_0|^2$: (a) $\theta_0 = 30^\circ$, (b) $\theta_0 = 60^\circ$ and (c) $\theta_0 = 80^\circ$ produced by a perforated 2D plasmonic layer of GaAs as a function of lateral distance $r_{//} = x(y = 0)$ from the aperture.

p - polarization: Far - Field, $z = 1000 R$; $\theta_0 = 30^\circ$

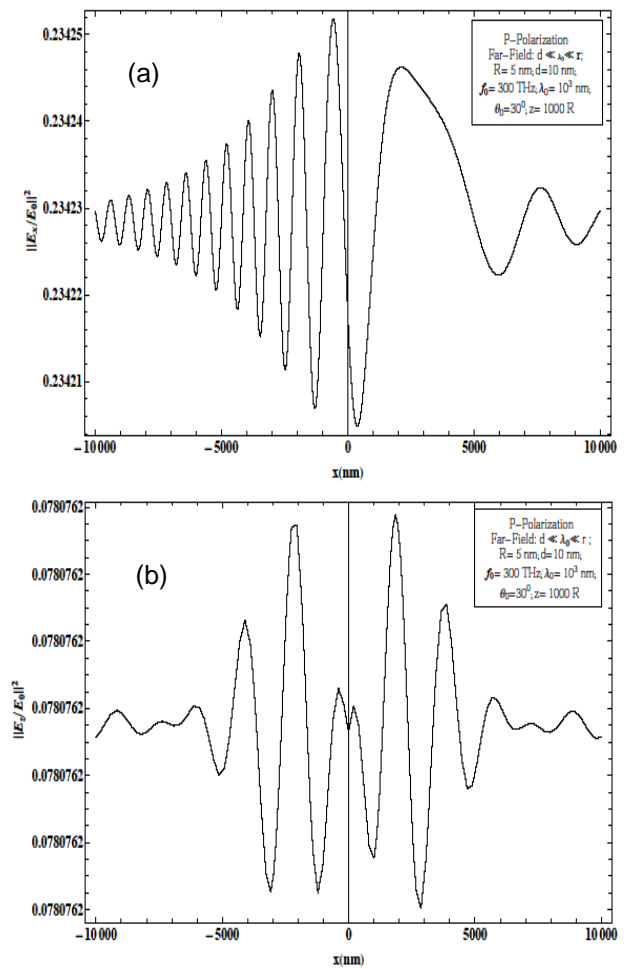


Fig.3.5. p - polarization - Far-Field, $z = 1000 R$; $\theta_0 = 30^\circ$: (a) $|E_x(x, y, z; t)/E_0|^2$ and (b) $|E_z(x, y, z; t)/E_0|^2$ produced by a perforated 2D plasmonic layer of GaAs as a function of lateral distance $r_{//} = x(y = 0)$ from the aperture.

Désiré Miessein, Norman J. M. Horing, Harry Lenzing, Godfrey Gumbs

Incident-Angle Dependence of EM Transmission Through a plasmonic Screen with a Nano-Aperture

ρ - polarization: Far - Field, $z = 1000 R$; $\theta_0 = 60^\circ$ ρ - polarization: Far - Field, $z = 1000 R$; $\theta_0 = 80^\circ$

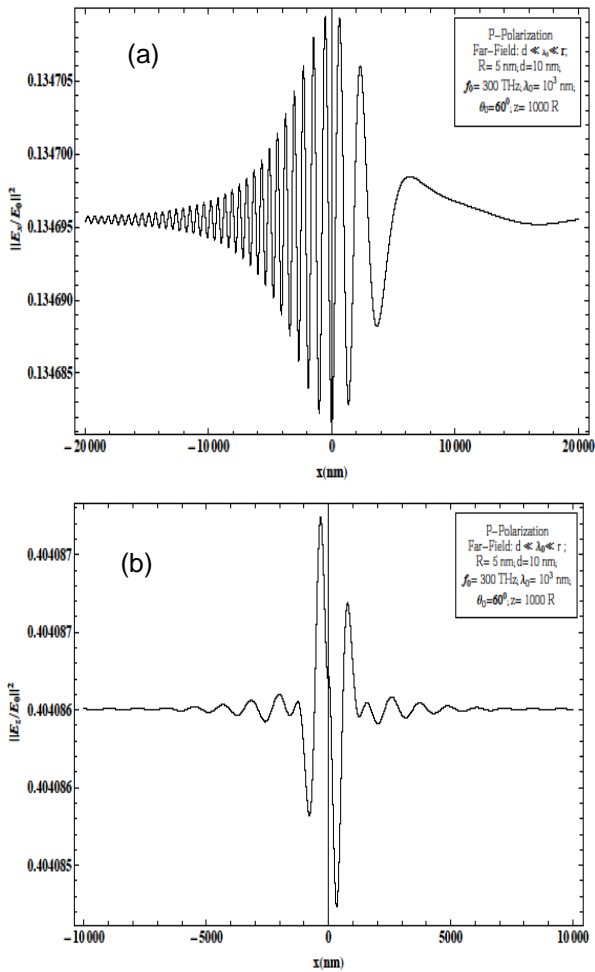


Fig.3.6. ρ - polarization - Far-Field, $z = 1000 R$; $\theta_0 = 60^\circ$: (a) $|E_x(x, y, z; t)/E_0|^2$ and (b) $|E_z(x, y, z; t)/E_0|^2$ produced by a perforated 2D plasmonic layer of GaAs as a function of lateral distance $r_{||} = x(y = 0)$ from the aperture.

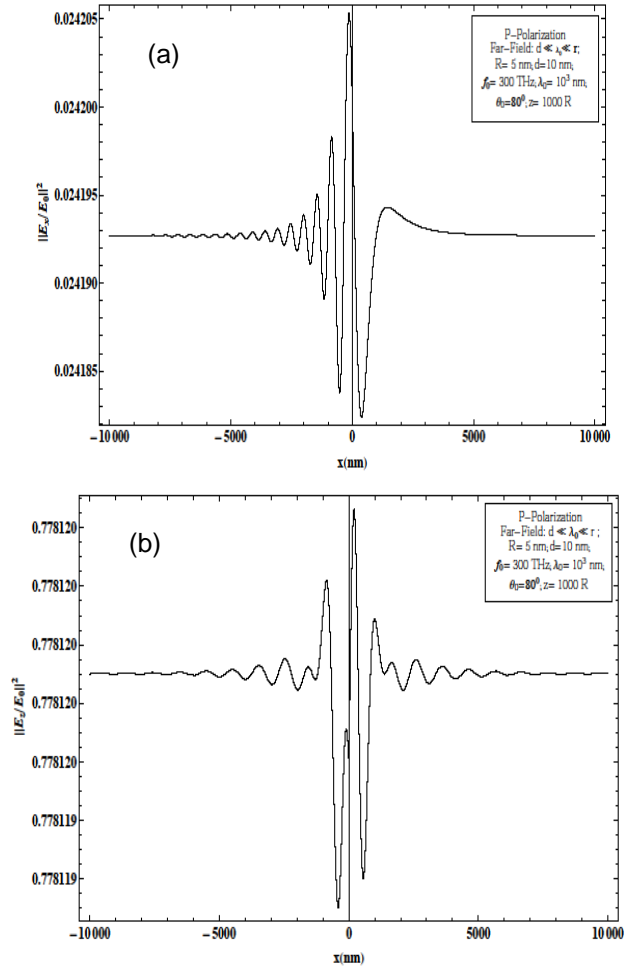


Fig.3.7. ρ - polarization - Far-Field, $z = 1000 R$; $\theta_0 = 80^\circ$: (a) $|E_x(x, y, z; t)/E_0|^2$ and (b) $|E_z(x, y, z; t)/E_0|^2$ produced by a perforated 2D plasmonic layer of GaAs as a function of lateral distance $r_{||} = x(y = 0)$ from the aperture.

Désiré Miessein, Norman J. M. Horing, Harry Lenzing, Godfrey Gumbs

Incident-Angle Dependence of EM Transmission Through a plasmonic Screen with a Nano-Aperture

s - polarization: Far - Field, $z = 1000 R$ p - polarization: Middle-Field, $z = 300 R$; $\theta_0 = 30^\circ$

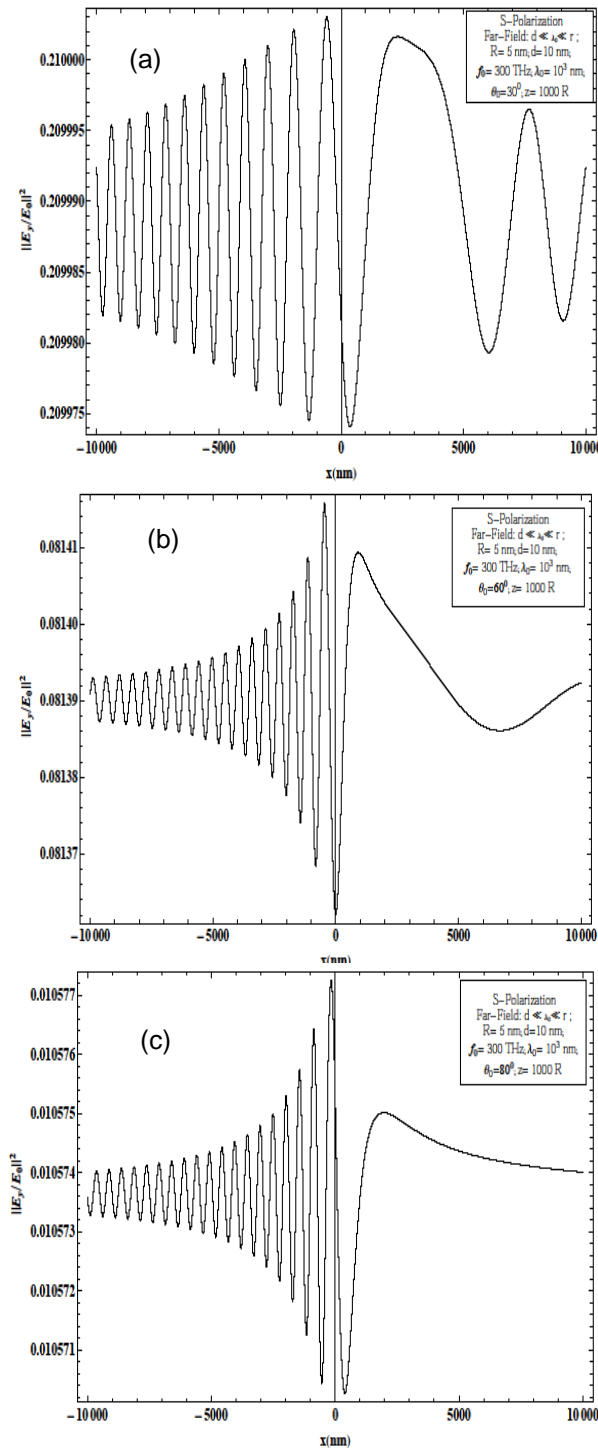


Fig.3.8. s - polarization-Middle - Field, $z = 1000 R$; $|E_y(x, y, z; t)/E_0|^2$: (a) $\theta_0 = 30^\circ$, (b) $\theta_0 = 60^\circ$ and (c) $\theta_0 = 80^\circ$ produced by a perforated 2D plasmonic layer of GaAs as a function of lateral distance $r_{||} = x(y = 0)$ from the aperture.

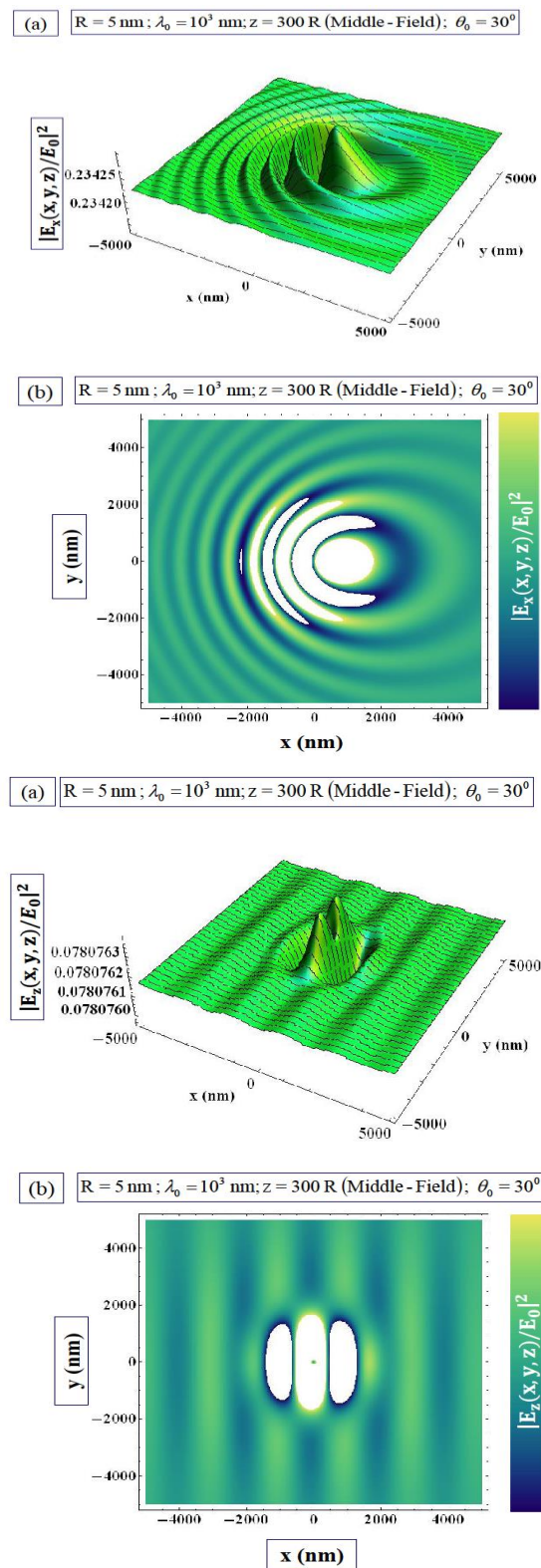


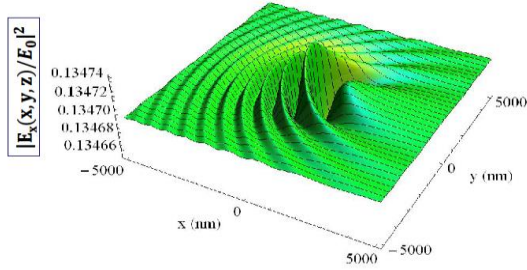
Fig. 3.9. p - polarization: Middle-Field, $z = 300 R$; $\theta_0 = 30^\circ$ - Field distribution of GaAs layer in terms of 3D (a's) and density (b's) plots: $|E_x(x, y, z; t)/E_0|^2$ and $|E_z(x, y, z; t)/E_0|^2$ as functions of x and y for fixed z .

Désiré Miessein, Norman J. M. Horing, Harry Lenzing, Godfrey Gumbs

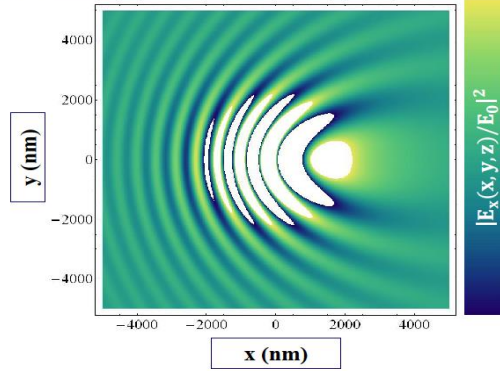
Incident-Angle Dependence of EM Transmission Through a plasmonic Screen with a Nano-Aperture

p - polarization: Middle-Field, $z = 300R$; $\theta_0 = 60^\circ$ **p - polarization: Middle-Field, $z = 300R$; $\theta_0 = 80^\circ$**

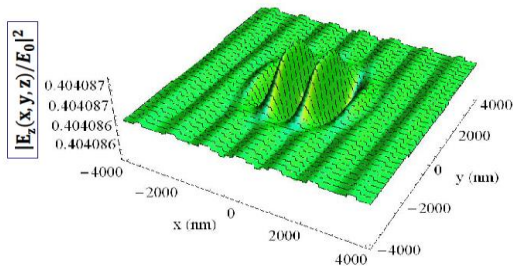
(a) $R = 5 \text{ nm}$; $\lambda_0 = 10^3 \text{ nm}$; $z = 300 R$ (Middle-Field); $\theta_0 = 60^\circ$



(b) $R = 5 \text{ nm}$; $\lambda_0 = 10^3 \text{ nm}$; $z = 300 R$ (Middle-Field); $\theta_0 = 60^\circ$



(a) $R = 5 \text{ nm}$; $\lambda_0 = 10^3 \text{ nm}$; $z = 300 R$ (Middle-Field); $\theta_0 = 60^\circ$



(b) $R = 5 \text{ nm}$; $\lambda_0 = 10^3 \text{ nm}$; $z = 300 R$ (Middle-Field); $\theta_0 = 60^\circ$

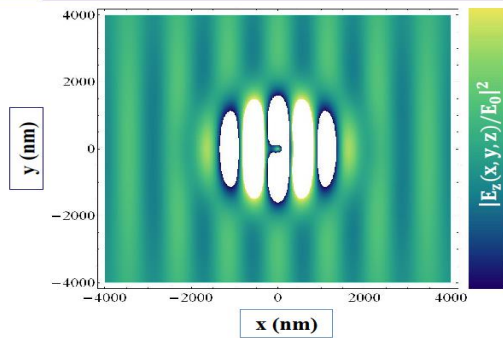
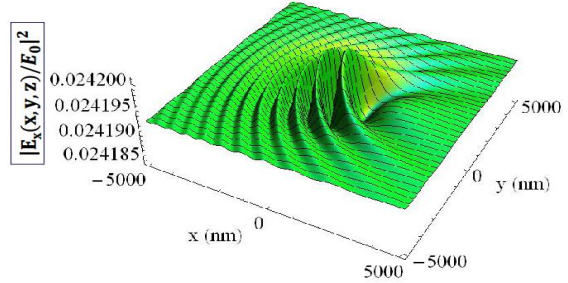
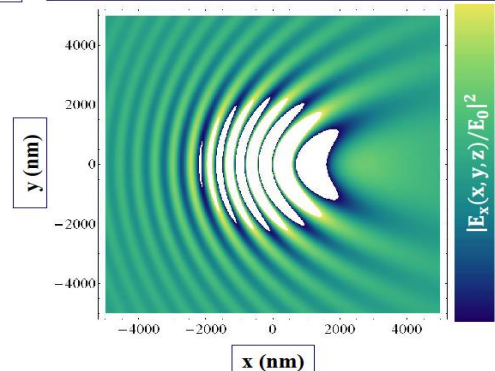


Fig. 3.10. p - polarization: Middle-Field, $z = 300R$; $\theta_0 = 60^\circ$ - Field distribution of GaAs layer in terms of 3D (a's) and density (b's) plots: $|E_x(x, y, z; t)/E_0|^2$ and $|E_z(x, y, z; t)/E_0|^2$ as functions of x and y for fixed z .

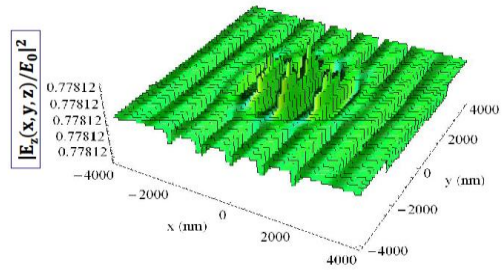
(a) $R = 5 \text{ nm}$; $\lambda_0 = 10^3 \text{ nm}$; $z = 300 R$ (Middle-Field); $\theta_0 = 80^\circ$



(b) $R = 5 \text{ nm}$; $\lambda_0 = 10^3 \text{ nm}$; $z = 300 R$ (Middle-Field); $\theta_0 = 80^\circ$



(a) $R = 5 \text{ nm}$; $\lambda_0 = 10^3 \text{ nm}$; $z = 300 R$ (Middle-Field); $\theta_0 = 80^\circ$



(b) $R = 5 \text{ nm}$; $\lambda_0 = 10^3 \text{ nm}$; $z = 300 R$ (Middle-Field); $\theta_0 = 80^\circ$

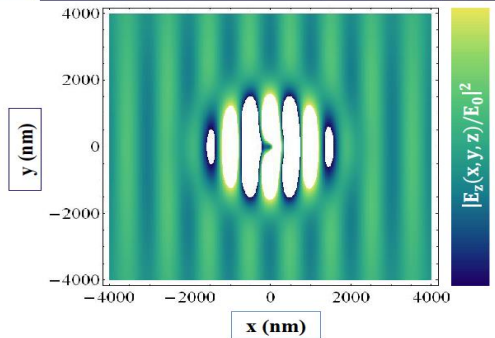


Fig. 3.11. p - polarization: Middle-Field, $z = 300R$; $\theta_0 = 80^\circ$ - Field distribution of GaAs layer in terms of 3D (a's) and density (b's) plots: $|E_x(x, y, z; t)/E_0|^2$ and $|E_z(x, y, z; t)/E_0|^2$ as functions of x and y for fixed z .

Désiré Miessein, Norman J. M. Horing, Harry Lenzing, Godfrey Gumbs

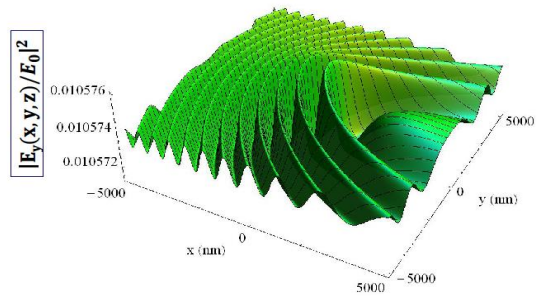
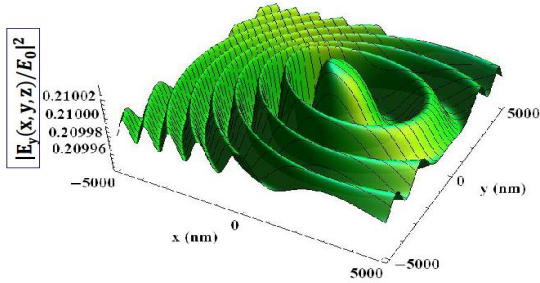
Incident-Angle Dependence of EM Transmission Through a plasmonic Screen with a Nano-Aperture

s - polarization: Middle-Field, $z = 300 R$

s - polarization: Middle-Field, $z = 300 R$

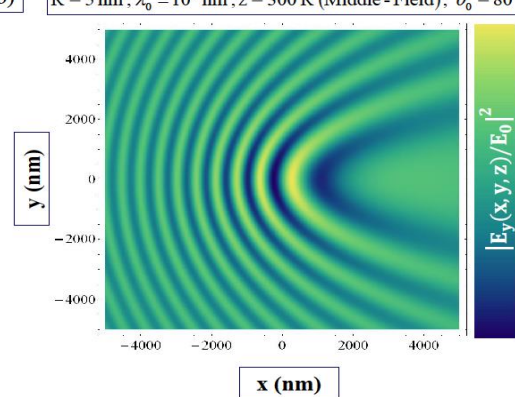
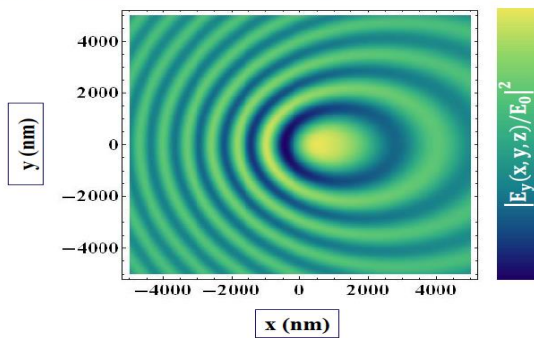
(a) $R = 5 \text{ nm}; \lambda_0 = 10^3 \text{ nm}; z = 300 R \text{ (Middle-Field)}; \theta_0 = 30^\circ$

(a) $R = 5 \text{ nm}; \lambda_0 = 10^3 \text{ nm}; z = 300 R \text{ (Middle-Field)}; \theta_0 = 80^\circ$

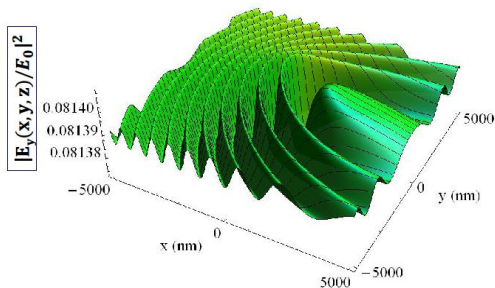


(b) $R = 5 \text{ nm}; \lambda_0 = 10^3 \text{ nm}; z = 300 R \text{ (Middle-Field)}; \theta_0 = 30^\circ$

(b) $R = 5 \text{ nm}; \lambda_0 = 10^3 \text{ nm}; z = 300 R \text{ (Middle-Field)}; \theta_0 = 80^\circ$



(a) $R = 5 \text{ nm}; \lambda_0 = 10^3 \text{ nm}; z = 300 R \text{ (Middle-Field)}; \theta_0 = 60^\circ$



(b) $R = 5 \text{ nm}; \lambda_0 = 10^3 \text{ nm}; z = 300 R \text{ (Middle-Field)}; \theta_0 = 60^\circ$

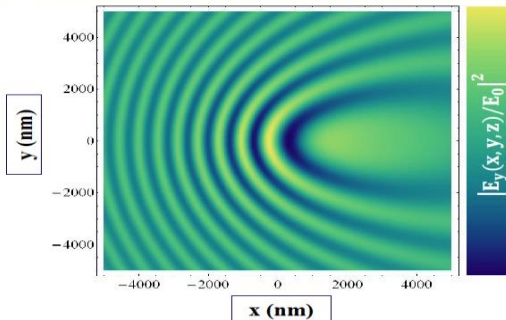


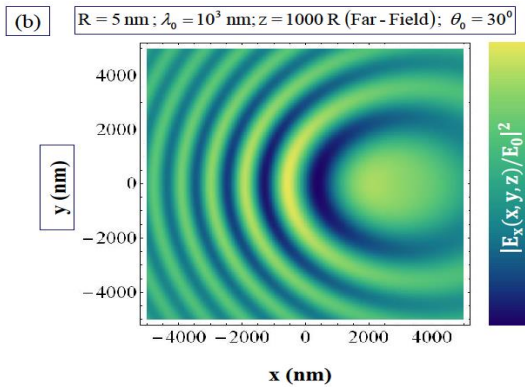
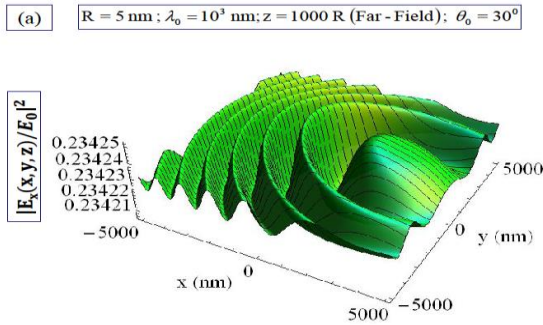
Fig.3.13. s - polarization: Middle-Field, $z = 300 R$ - Field distribution of GaAs layer in terms of 3D (a's) and density (b's) plots: $|E_y(x, y, z; t)/E_0|^2$ (a) $\theta_0 = 80^\circ$, and (b) $\theta_0 = 80^\circ$ as functions of x and y for fixed z .

Fig.3.12. s - polarization: Middle-Field, $z = 300 R$ - Field distribution of GaAs layer in terms of 3D (a's) and density (b's) plots: $|E_y(x, y, z; t)/E_0|^2$ (a) $\theta_0 = 30^\circ, 60^\circ$ and (b) $\theta_0 = 30^\circ, 60^\circ$ as functions of x and y for fixed z .

Désiré Miessein, Norman J. M. Horing, Harry Lenzing, Godfrey Gumbs

Incident-Angle Dependence of EM Transmission Through a plasmonic Screen with a Nano-Aperture

p - polarization: Far-Field, $z = 1000 R; \theta_0 = 30^\circ$



(a) $R = 5 \text{ nm}; \lambda_0 = 10^3 \text{ nm}; z = 1000 R \text{ (Far - Field)}; \theta_0 = 30^\circ$

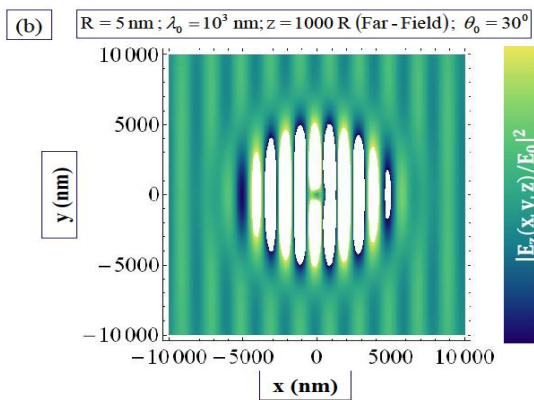
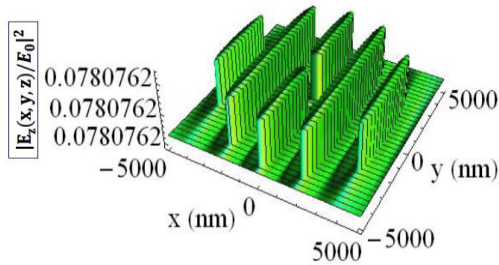
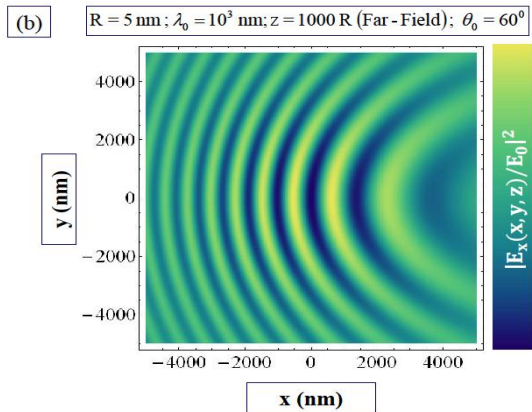
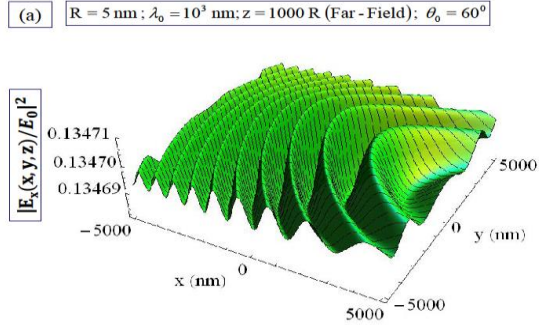


Fig.3.14. p - polarization: Far-Field, $z = 10^3 R; \theta_0 = 30^\circ$ - Field distribution of GaAs layer in terms of 3D (a's) and density (b's) plots: $|E_x(x, y, z; t)/E_0|^2$ and $|E_z(x, y, z; t)/E_0|^2$ as functions of x and y for fixed z.

p - polarization: Far-Field, $z = 1000 R; \theta_0 = 60^\circ$



(a) $R = 5 \text{ nm}; \lambda_0 = 10^3 \text{ nm}; z = 1000 R \text{ (Far - Field)}; \theta_0 = 60^\circ$

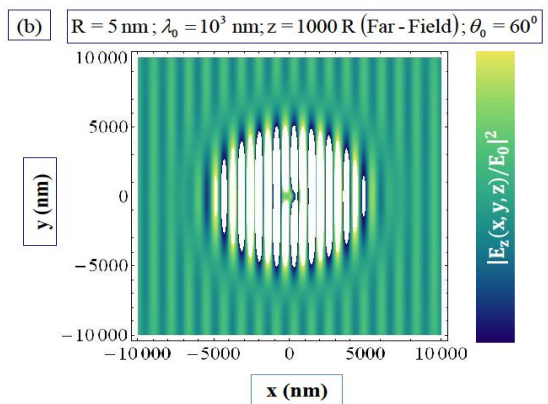
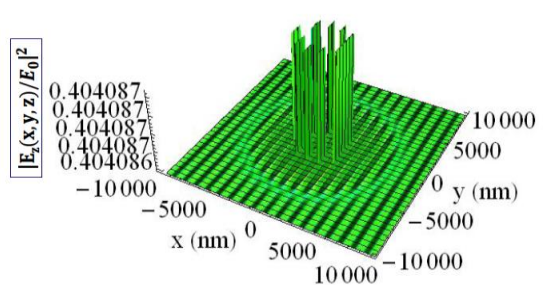


Fig.3.15. p - polarization: Far-Field, $z = 10^3 R; \theta_0 = 60^\circ$ - Field distribution of GaAs layer in terms of 3D (a's) and density (b's) plots: $|E_x(x, y, z; t)/E_0|^2$ and $|E_z(x, y, z; t)/E_0|^2$ as functions of x and y for fixed z.

Désiré Miessein, Norman J. M. Horing, Harry Lenzing, Godfrey Gumbs

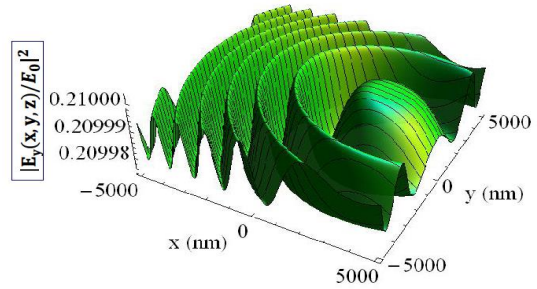
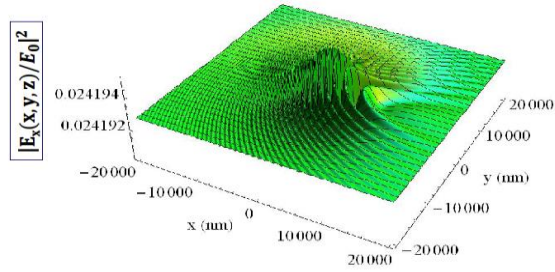
Incident-Angle Dependence of EM Transmission Through a plasmonic Screen with a Nano-Aperture

p - polarization: Far-Field, $z = 1000 R$; $\theta_0 = 80^\circ$

s - polarization: Far-Field, $z = 1000 R$;

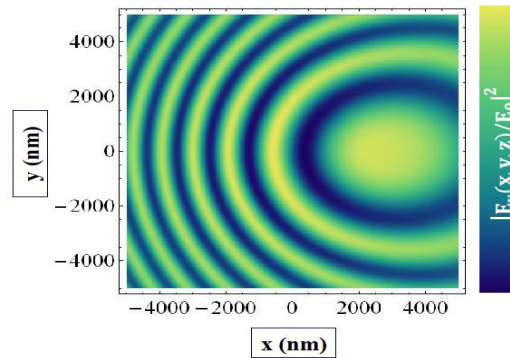
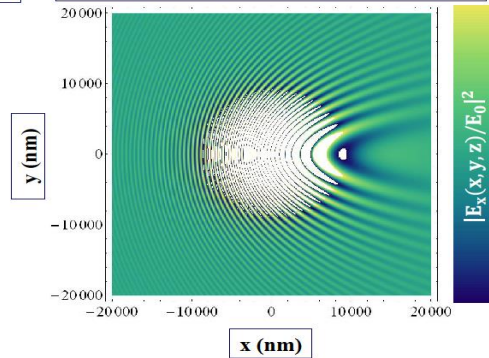
(a) $R = 5 \text{ nm}; \lambda_0 = 10^3 \text{ nm}; z = 1000 R \text{ (Far-Field)}; \theta_0 = 80^\circ$

(a) $R = 5 \text{ nm}; \lambda_0 = 10^3 \text{ nm}; z = 1000 R \text{ (Far-Field)}; \theta_0 = 30^\circ$



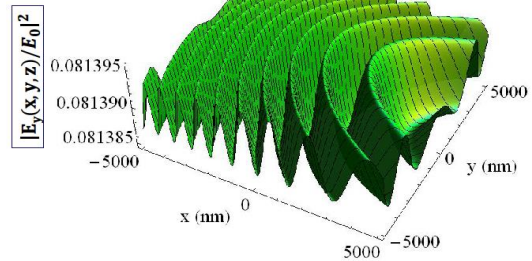
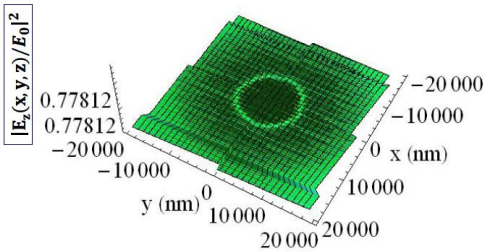
(b) $R = 5 \text{ nm}; \lambda_0 = 10^3 \text{ nm}; z = 1000 R \text{ (Far-Field)}; \theta_0 = 80^\circ$

(b) $R = 5 \text{ nm}; \lambda_0 = 10^3 \text{ nm}; z = 1000 R \text{ (Far-Field)}; \theta_0 = 30^\circ$



(a) $R = 5 \text{ nm}; \lambda_0 = 10^3 \text{ nm}; z = 1000 R \text{ (Far-Field)}; \theta_0 = 80^\circ$

(a) $R = 5 \text{ nm}; \lambda_0 = 10^3 \text{ nm}; z = 1000 R \text{ (Far-Field)}; \theta_0 = 60^\circ$



(b) $R = 5 \text{ nm}; \lambda_0 = 10^3 \text{ nm}; z = 1000 R \text{ (Far-Field)}; \theta_0 = 80^\circ$

(b) $R = 5 \text{ nm}; \lambda_0 = 10^3 \text{ nm}; z = 1000 R \text{ (Far-Field)}; \theta_0 = 60^\circ$

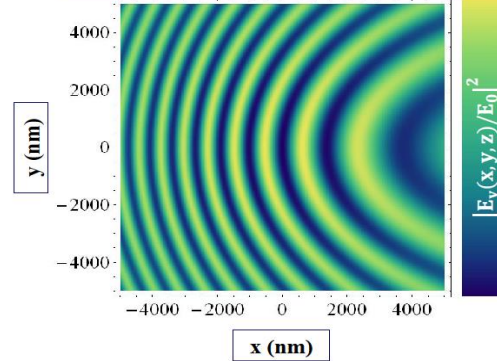
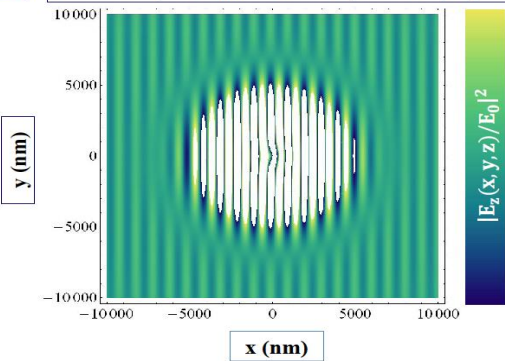


Fig.3.16. p - polarization: Far-Field, $z = 10^3 R$; $\theta_0 = 80^\circ$ - Field distribution of GaAs layer in terms of 3D (a's) and density (b's) plots: $|E_x(x, y, z; t)/E_0|^2$ and $|E_z(x, y, z; t)/E_0|^2$ as functions of x and y for fixed z .

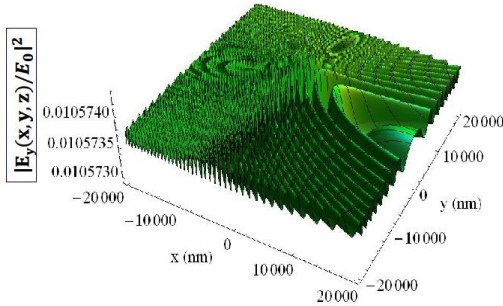
Fig.3.17. s - polarization: Far-Field, $z = 10^3 R$ - Field distribution of GaAs layer in terms of 3D (a's) and density (b's) plots: $|E_y(x, y, z; t)/E_0|^2$ (a) $\theta_0 = 30^\circ, 60^\circ$ and (b) $\theta_0 = 30^\circ, 60^\circ$ as functions of x and y for fixed z .

Désiré Miessein, Norman J. M. Horing, Harry Lenzing, Godfrey Gumbs

Incident-Angle Dependence of EM Transmission Through a plasmonic Screen with a Nano-Aperture

s - polarization: Far-Field, $z = 1000 R$;

(a) $R = 5 \text{ nm}; \lambda_0 = 10^3 \text{ nm}; z = 1000 R \text{ (Far-Field)}; \theta_0 = 80^\circ$



(b) $R = 5 \text{ nm}; \lambda_0 = 10^3 \text{ nm}; z = 1000 R \text{ (Far-Field)}; \theta_0 = 80^\circ$

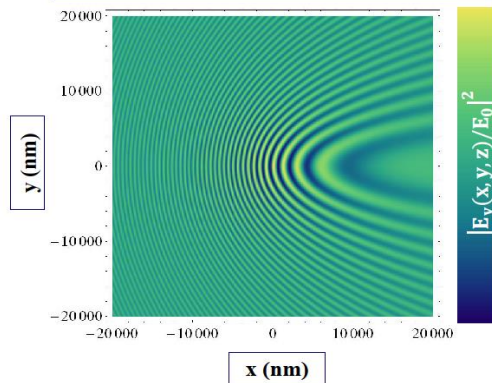


Fig.3.18. s - polarization: Far-Field, $z = 10^3 R$ - Field distribution of GaAs layer in terms of 3D (a's) and density (b's) plots: $|E_y(x, y, z; t)/E_0|^2$ (a) $\theta_0 = 80^\circ$ and (b) $\theta_0 = 80^\circ$ as functions of x and y for fixed z

4. Conclusions

In this work we have explored the role of *non-normal* angles of incidence on the transmission of an electromagnetic wave train through a nano-hole in a thin plasmonic semiconductor screen. This study is based on our previously constructed [1-5] closed-form dyadic electromagnetic Green's function for a thin plasmonic/excitonic layer adapted to embody a nano-hole. The resulting closed-form dyadic Green's function encompasses electromagnetic wave transmission through both the hole as well as through the screen itself. This analytic approach involving closed-form solutions of associated integral equations has facilitated the relatively simple numerical computations exhibited above, and is not in any way restricted to an ideal metallic screen. Moreover, our formulation, which is based on the use of an *integral* equation for the dyadic Green's function involved automatically incorporates the boundary conditions,

which would otherwise need to be addressed explicitly. It also incorporates the role of the two dimensional plasmon of the thin layer, which is smeared by its lateral wavenumber dependence.

The calculated results shown in the figures of Section III contrast sharply with the corresponding figures for normal incidence. Even for the lowest incident angle of 30° considered in the case of p-polarization, the results are highly asymmetric in x (while the corresponding results for normal incidence are symmetric) [1]. Such strong asymmetry persists at higher angles of incidence considered ($60^\circ; 80^\circ$), as may be seen in Figs.3.1-3.8 for p-polarization and s-polarization. Further supporting 3D and density plots are given in Figs.3.9 - 3.18 for the various angles of incidence and polarizations in the spatial zones considered.

All of the figures exhibit interference fringes due to the superposition of the field transmitted through the nano-hole with the field transmitted *directly* through the plasmonic sheet. At large distances from the nano-hole, the transmission directly through the plasmonic sheet dominates, and the interference fringes flatten to a uniform level of transmission through the sheet alone, with the nano-hole contribution negligible.

Finally, it should be noted that the figures show that as the incident angle increases, the axis of the relatively large central transmission maximum follows it generating greater asymmetry accompanied by a spatial compression of interference fringe maxima forward of the large central transmission maximum and a spatial thinning of the fringe maxima behind it. Moreover, while there is strong asymmetry of electromagnetic transmission with respect to the x -axis (of the $x - z$ plane of incidence), it should be borne in mind that the transmission is fully symmetric with respect to the y -axis (normal to the plane of incidence). Furthermore, the *p*-polarization transmission results show strong increase as incident angle θ_0 increases, mainly in the E_z component.

Appendix A: Matrix Elements of $\hat{\Omega}^{-1}$ and $\hat{G}_{3D}(\vec{k}_{//}; z, 0; \omega)$

The elements of $\hat{\Omega}^{-1}$ are given by (notation: $a_0^2 = k_z^2 - 2ik_z/d$)

Désiré Miessein, Norman J. M. Horing, Harry Lenzing, Godfrey Gumbs

Incident-Angle Dependence of EM Transmission Through a plasmonic Screen with a Nano-Aperture

$$[\hat{\Omega}^{-1}]_{11} = \frac{\left[1 + \left(\frac{\gamma}{2ik_z}\right)\left(1 - \frac{k_y^2}{q_\omega^2}\right)\right]}{\left[\left(1 + \left(\frac{\gamma}{2ik_z}\right)\right)\left(1 + \left(\frac{\gamma}{2ik_z}\right)\left(1 - \frac{k_{//}^2}{q_\omega^2}\right)\right)\right]}, \quad (33) \quad G_{3D}^{xz}(\vec{k}_{//}; z, 0; \omega) = + \frac{e^{ik_z|z|}}{2ik_z} \left(\frac{k_x k_z \operatorname{sgn}(z)}{q_\omega^2}\right), \quad (43)$$

$$[\hat{\Omega}^{-1}]_{12} = \frac{\left[\left(\frac{\gamma}{2ik_z}\right)\left(\frac{k_x k_y}{q_\omega^2}\right)\right]}{\left[\left(1 + \left(\frac{\gamma}{2ik_z}\right)\right)\left(1 + \left(\frac{\gamma}{2ik_z}\right)\left(1 - \frac{k_{//}^2}{q_\omega^2}\right)\right)\right]}, \quad (34) \quad G_{3D}^{yz}(\vec{k}_{//}; z, 0; \omega) = + \frac{e^{ik_z|z|}}{2ik_z} \left(\frac{k_y k_z \operatorname{sgn}(z)}{q_\omega^2}\right), \quad (44)$$

$$[\hat{\Omega}^{-1}]_{21} = [\hat{\Omega}^{-1}]_{12}, \quad (35) \quad G_{3D}^{yx}(\vec{k}_{//}; z, 0; \omega) = G_{3D}^{xy}(\vec{k}_{//}; z, 0; \omega), \quad (45)$$

$$[\hat{\Omega}^{-1}]_{31} = [\hat{\Omega}^{-1}]_{13} = [\hat{\Omega}^{-1}]_{32} = [\hat{\Omega}^{-1}]_{23} = 0, \quad (36) \quad G_{3D}^{xz}(\vec{k}_{//}; z, 0; \omega) = G_{3D}^{zx}(\vec{k}_{//}; z, 0; \omega), \quad (46)$$

$$[\hat{\Omega}^{-1}]_{22} = \frac{\left[1 + \left(\frac{\gamma}{2ik_z}\right)\left(1 - \frac{k_x^2}{q_\omega^2}\right)\right]}{\left[\left(1 + \left(\frac{\gamma}{2ik_z}\right)\right)\left(1 + \left(\frac{\gamma}{2ik_z}\right)\left(1 - \frac{k_{//}^2}{q_\omega^2}\right)\right)\right]}, \quad (37) \quad G_{3D}^{yz}(\vec{k}_{//}; z, 0; \omega) = G_{3D}^{zy}(\vec{k}_{//}; z, 0; \omega). \quad (47)$$

and

$$[\hat{\Omega}^{-1}]_{33} = \frac{1}{\left[1 + \left(\frac{\gamma}{2ik_z}\right)\left(1 - \frac{a_0^2}{q_\omega^2}\right)\right]}. \quad (38) \quad \text{Therefore, Eq.(16) may be rewritten as}$$

Appendix B:

Furthermore the elements of $\hat{G}_{3D}(\vec{k}_{//}; z, 0; \omega)$ are given by the matrix $G_{3D}^{ij}(\vec{k}_{//}; z, 0; \omega)$ as:

$$G_{3D}^{xx}(\vec{k}_{//}; z, 0; \omega) = - \frac{e^{ik_z|z|}}{2ik_z} \left(1 - \frac{k_x^2}{q_\omega^2}\right), \quad (39)$$

$$G_{3D}^{yy}(\vec{k}_{//}; z, 0; \omega) = - \frac{e^{ik_z|z|}}{2ik_z} \left(1 - \frac{k_y^2}{q_\omega^2}\right), \quad (40)$$

$$G_{3D}^{zz}(\vec{k}_{//}; z, 0; \omega) = - \frac{e^{ik_z|z|}}{2ik_z} \times \left(1 - \frac{k_z^2 - 2ik_z \delta(z)}{q_\omega^2}\right), \quad (41)$$

$$G_{3D}^{xy}(\vec{k}_{//}; z, 0; \omega) = + \frac{e^{ik_z|z|}}{2ik_z} \left(\frac{k_x k_y}{q_\omega^2}\right), \quad (42)$$

Appendix C: Matrix Elements of $\hat{G}_{fs} \mapsto$

$$G_{fs}^{ij}(\vec{k}_{//}; z, 0; \omega) = - \frac{e^{ik_z|z|}}{2ik_z} \times \left[\frac{1}{D_1} \left\{ \left(1 - \frac{k_x^2}{q_\omega^2}\right) + \left(\frac{\gamma}{2ik_z}\right) \left(1 - \frac{k_{//}^2}{q_\omega^2}\right) \right\}\right], \quad (49)$$

$$G_{fs}^{yy}(\vec{k}_{//}; z, 0; \omega) = - \frac{e^{ik_z|z|}}{2ik_z} \times \left[\frac{1}{D_1} \left\{ \left(1 - \frac{k_y^2}{q_\omega^2}\right) + \left(\frac{\gamma}{2ik_z}\right) \left(1 - \frac{k_{//}^2}{q_\omega^2}\right) \right\}\right], \quad (50)$$

$$G_{fs}^{zz}(\vec{k}_{//}; z, 0; \omega) = - \frac{e^{ik_z|z|}}{2ik_z} \times \left[\frac{1}{D_2} \left\{ \left(1 - \frac{k_z^2 - 2ik_z \delta(z)}{q_\omega^2}\right) \right\}\right], \quad (51)$$

$$G_{fs}^{xy}(\vec{k}_{//}; z, 0; \omega) = + \frac{e^{ik_z|z|}}{2ik_z} \left[\frac{1}{D_1} \left(\frac{k_x k_y}{q_\omega^2}\right)\right], \quad (52)$$

$$G_{fs}^{xz}(\vec{k}_{//}; z, 0; \omega) = + \frac{e^{ik_z|z|}}{2ik_z} \left[\frac{1}{D_2} \left(\frac{k_x k_z \operatorname{sgn}(z)}{q_\omega^2}\right)\right], \quad (53)$$

$$G_{fs}^{yz}(\vec{k}_{//}; z, 0; \omega) = + \frac{e^{ik_z|z|}}{2ik_z} \left[\frac{1}{D_2} \left(\frac{k_y k_z \operatorname{sgn}(z)}{q_\omega^2}\right)\right], \quad (54)$$

$$G_{fs}^{yx}(\vec{k}_{//}; z, 0; \omega) = G_{fs}^{xy}(\vec{k}_{//}; z, 0; \omega), \quad (55)$$

$$G_{fs}^{zx}(\vec{k}_{//}; z, 0; \omega) = - \frac{e^{ik_z|z|}}{2ik_z} \times \left[\frac{1}{D_1} \left\{ \left(1 + \left(\frac{\gamma}{2ik_z}\right)\right) \frac{k_z k_x \operatorname{sgn}(z)}{q_\omega^2} \right\}\right], \quad (56)$$

Désiré Miessein, Norman J. M. Horing, Harry Lenzing, Godfrey Gumbs

Incident-Angle Dependence of EM Transmission Through a plasmonic Screen with a Nano-Aperture

$$G_{fs}^{zy}(\vec{k}_{//}; z, 0; \omega) = -\frac{e^{ik_z|z|}}{2ik_z} \times \left[\frac{1}{D_1} \left\{ 1 + \left(\frac{\gamma}{2ik_z} \right) \frac{k_z k_y \text{sgn}(z)}{q_\omega^2} \right\} \right], \quad (57)$$

$$G_{fs}^{xz}(\vec{k}_{//}; z, 0; \omega) = G_{fs}^{zx}(\vec{k}_{//}; z, 0; \omega), \quad (58)$$

and

$$D_1 = \left[1 + \left(\frac{\gamma}{2ik_z} \right) \right] \left[1 + \left(\frac{\gamma}{2ik_z} \right) \left(1 - \frac{k_{//}^2}{q_\omega^2} \right) \right], \quad (59)$$

$$D_2 = \left[1 + \left(\frac{\gamma}{2ik_z} \right) \left(1 - \frac{q_0^2}{q_\omega^2} \right) \right]. \quad (60)$$

It should be noted that, in the text above, we choose the coordinate system such that $k_y \equiv 0$. In this case $k_{//} = k_x$ and $k_z^2 = q_\omega^2 - k_x^2$. Moreover, with $k_y = 0$, $\hat{G}_{3D}(\vec{k}_{//}; 0, 0; \omega)$ becomes diagonal.

Appendix D: Matrix Elements of \hat{T}^0

Since $\hat{G}_{fs}(\vec{k}_{0//}; 0, 0; \omega_0) \equiv \hat{G}_{fs}$ is diagonal, we have (notation: $\hat{G} \equiv \hat{G}(\vec{r}_{//}; 0, z, 0; \omega_0)$ here)

$$\hat{T}^0 = \begin{bmatrix} G^{xx} & 0 & G^{xz} \\ 0 & G^{yy} & 0 \\ G^{zx} & 0 & G^{zz} \end{bmatrix} \times \begin{bmatrix} 1 + \gamma_0 \bar{G}_{fs}^{xx} & 0 & 0 \\ 0 & 1 + \gamma_0 \bar{G}_{fs}^{yy} & 0 \\ 0 & 0 & 1 + \gamma_0 \bar{G}_{fs}^{zz} \end{bmatrix} \quad (61)$$

or

$$\hat{T}^0 = \begin{bmatrix} T_{xx}^0 & 0 & T_{xz}^0 \\ 0 & T_{yy}^0 & 0 \\ T_{zx}^0 & 0 & T_{zz}^0 \end{bmatrix} \quad (62)$$

where the matrix elements are given by

$$\begin{cases} T_{xx}^0 = G^{xx} \left[1 + \gamma_0 \bar{G}_{fs}^{xx} \right]; & (a) \\ T_{zx}^0 = G^{zx} \left[1 + \gamma_0 \bar{G}_{fs}^{xx} \right]; & (b) \\ T_{yy}^0 = G^{yy} \left[1 + \gamma_0 \bar{G}_{fs}^{yy} \right]; & (c) \\ T_{xz}^0 = G^{xz} \left[1 + \gamma_0 \bar{G}_{fs}^{zz} \right]; & (d) \\ T_{zz}^0 = G^{zz} \left[1 + \gamma_0 \bar{G}_{fs}^{zz} \right]. & (e) \end{cases} \quad (63)$$

In order to facilitate the calculations of the above matrix elements, it is important to note that $\hat{G} \equiv \hat{G}(\vec{r}_{//}; 0, z, 0; \omega_0)$ and $\bar{G}_{fs} \equiv \bar{G}_{fs}(\vec{k}_{0//}; 0, 0; \omega_0)$ are evaluated at the incident wave frequency ω_0 . Therefore, the matrix elements of the dyad \hat{T}^0 are given by (note that θ_0 is the angle of incident)

$$T_{xx}^0 = G_{fs}^{xx} \left[\frac{1 + \gamma_0 \bar{G}_{fs}^{xx}}{1 + \beta_0 G_{fs_0}^{xx}} \right] \quad (64)$$

where

$$\begin{cases} \bar{G}_{fs}^{xx} \equiv \frac{-\cos(\theta_0)}{2i \left[q_{\omega_0} + \Gamma_0 \cos(\theta_0) \right]}; & (a) \\ G_{fs_0}^{xx} \equiv G_{fs_0}^{xx}(0-0; 0, 0; \omega_0); & (b) \\ G_{fs}^{xx} \equiv G_{fs}^{xx}(\vec{r}_{//}; 0; z, 0; \omega_0). & (c) \end{cases} \quad (65)$$

$$T_{yy}^0 = G_{fs}^{yy} \left[\frac{1 + \gamma_0 \bar{G}_{fs}^{yy}}{1 + \beta_0 G_{fs_0}^{yy}} \right] \quad (66)$$

where

$$\begin{cases} \bar{G}_{fs}^{yy} \equiv \frac{-1}{2i \left[\Gamma_0 + q_{\omega_0} \cos(\theta_0) \right]}; & (a) \\ G_{fs_0}^{yy} \equiv G_{fs_0}^{yy}(0-0; 0, 0; \omega_0); & (b) \\ G_{fs}^{yy} \equiv G_{fs}^{yy}(\vec{r}_{//}; 0; z, 0; \omega_0). & (c) \end{cases} \quad (67)$$

$$T_{zz}^0 = G_{fs}^{zz} \left[\frac{1 + \gamma_0 \bar{G}_{fs}^{zz}}{1 + \beta_0 G_{fs_0}^{zz}} \right] \quad (68)$$

where

$$\begin{cases} \bar{G}_{fs}^{zz} \equiv \frac{-1}{2i} \left\{ \frac{q_{\omega_0} \sin^2(\theta_0) + 2i\delta(0)\cos(\theta_0)}{\cos(\theta_0) \left[q_{\omega_0}^2 + 2i\delta(0)\Gamma_0 \right] + q_{\omega_0} \Gamma_0 \sin^2(\theta_0)} \right\}; & (a) \\ G_{fs_0}^{zz} \equiv G_{fs_0}^{zz}(0-0; 0, 0; \omega_0); & (b) \\ G_{fs}^{zz} \equiv G_{fs}^{zz}(\vec{r}_{//}; 0; z, 0; \omega_0). & (c) \end{cases} \quad (69)$$

$$T_{xz}^0 = G_{fs}^{xz} \left[\frac{1 + \gamma_0 \bar{G}_{fs}^{zz}}{1 + \beta_0 G_{fs_0}^{zz}} \right] \quad (70)$$

where

$$\begin{cases} \bar{G}_{fs}^{zz} \equiv \frac{-1}{2i} \left\{ \frac{q_{\omega_0} \sin^2(\theta_0) + 2i\delta(0)\cos(\theta_0)}{\cos(\theta_0) \left[q_{\omega_0}^2 + 2i\delta(0)\Gamma_0 \right] + q_{\omega_0} \Gamma_0 \sin^2(\theta_0)} \right\}; & (a) \\ G_{fs_0}^{zz} \equiv G_{fs_0}^{zz}(0-0; 0, 0; \omega_0); & (b) \\ G_{fs}^{xz} \equiv G_{fs}^{xz}(\vec{r}_{//}; 0; z, 0; \omega_0). & (c) \end{cases} \quad (71)$$

and

$$T_{zx}^0 = G_{fs}^{zx} \left[\frac{1 + \gamma_0 \bar{G}_{fs}^{xx}}{1 + \beta_0 G_{fs_0}^{xx}} \right] \quad (72)$$

where

$$\begin{cases} \bar{G}_{fs}^{xx} \equiv \frac{-\cos(\theta_0)}{2i \left[q_{\omega_0} + \Gamma_0 \cos(\theta_0) \right]}; & (a) \\ G_{fs_0}^{xx} \equiv G_{fs_0}^{xx}(0-0; 0, 0; \omega_0); & (b) \\ G_{fs}^{zx} \equiv G_{fs}^{zx}(\vec{r}_{//}; 0; z, 0; \omega_0). & (c) \end{cases} \quad (73)$$

Désiré Miessein, Norman J. M. Horing, Harry Lenzing, Godfrey Gumbs

Incident-Angle Dependence of EM Transmission Through a plasmonic Screen with a Nano-Aperture

Acknowledgements

Dr. Désiré Miessein gratefully acknowledges support by the AGEP program of the NSF; also the assistance of Prof. M. L. Glasser, Dr. Andrii Iurov and Dr. Nan Chen

References

- [1] Horing N. J. M., Miessein D. and Gumbs G. Electromagnetic wave transmission through a subwavelength nano-hole in a two-dimensional plasmonic layer J. Opt. Soc. Am. A 32 1184-8 (2015).
- [2] Miessein D. Scalar and Electromagnetic Waves Transmission Through a Subwavelength Nano-hole in a 2D Plasmonic Semiconductor Layer Ph.D Thesis Stevens Institute of Technology, Hoboken, New Jersey (2013).
- [3] Horing N. J. M., Bagaeva T. Y. and Popov V. V. Excitation of radiative polaritons in a two-dimensional excitonic layer by a light pulse J. Opt. Soc. Am. B 24, 2428-35 (2007).
- [4] Horing N. J. M. Quantum Statistical Field Theory: Schwinger's Variational Method Oxford University Press in press (2015).
- [5] Horing N. J. M. Radiative Plasmonic-Polariton Dispersion Relation for a Thin Metallic Foil With Interband Damping Transitions IEEE Sensors J. 8, 771-4 (2008).
- [6] Bethe H. A. Theory of Diffraction by Small Holes Phys. Rev. 66, 163-182 (1944).
- [7] Bouwkamp C. J. On Bethe's Theory of Diffraction by Small Holes Philips Res. Rep. 5, 321-332 (1950).
- [8] Levine H. and Schwinger J. On the theory of electromagnetic wave diffraction by an aperture in an infinite plane conducting screen Commun. Pure and Appl. Math. 3, 355-391 (1950).
- [9] Levine H. and Schwinger J. On the Theory of Diffraction by an Aperture in an Infinite Plane Screen I Phys. Rev. 74, 958-974 (1948).
- [10] Levine H. and Schwinger J. On the Theory of Diffraction by an Aperture in an Infinite Plane Screen II Phys. Rev. 75 1423-1432 (1949).
- [11] Tai Chen-To Dyadic Green's Functions in Electromagnetic Theory (Piscataway, NJ: IEEE) (1994).
- [12] Tai Chen-To General Vector and Dyadic Analysis: Applied Mathematics in Field Theory (Hoboken, NJ: Wiley-IEEE Press) (1997).
- [13] Collin R. E. Field Theory of Guided Waves (Piscataway, NJ: IEEE) (1991).
- [14] Chew W.C. Waves and Fields In Inhomogeneous Media (Piscataway, NJ: IEEE) (1995).
- [15] Ebbesen T. W., Lezec H. J., Ghaemi H. F., Thio T. and Wolff P. A. Extraordinary optical transmission through sub-wavelength hole arrays Nature, 391, 667-669 (1998).
- [16] Garcia-Vidal F. J., Martin-Moreno L., Ebbesen T. W. and Kuiperd L. Light passing through subwavelength apertures Rev. Mod. Phys. 82, 729-787(2010).
- [17] Neerhoff F. L. and Mur G. Diffraction of a plane electromagnetic wave by a slit in a thick screen placed between two different media Appl. Sci. Res. 28, 73-88 (1973).
- [18] Gradshteyn I. S. and Ryzhik M. I. Table of Integrals, Series, and Products, 6th Ed (New York: Academic Press) (1980).
- [19] Leviatan Y. Study of Near-zone Field of a Small Aperture J. Appl. Phys. 60 1577-1583 (1986).
- [20] Roberts A. Near-zone Fields Behind Circular Apertures in Thick, Perfectly Conducting Screens J. Appl. Phys. 65 2896-2899 (1988).
- [21] Wannemacher R. Plasmon-supported transmission of light through nanometric holes in metallic thin films Opt. Commun. 195 107-118 (2001).

Désiré Miessein, Norman J. M. Horing, Harry Lenzing, Godfrey Gumbs

Incident-Angle Dependence of EM Transmission Through a plasmonic Screen with a Nano-Aperture

- [22] Arnoldus H. F. and Foley J. T. Traveling and evanescent parts of the electromagnetic Green's tensor J. Optical Soc. Amer. A 19 1701 (2002).
- [23] Garcia de Abajo F. J. Light transmission through a single cylindrical hole in a metallic film Opt. Express 10 1475-1484 (2002).
- [24] Shi X. Hesselink L. Thornton R. L. Ultrahigh light transmission through a C-shaped nanoaperture Opt. Letters 28, 1320-1322 (2003).
- [25] Kulkhlevsky S. V., Mechler M., Csapo L., Janssens K., and O. Samek Enhanced transmission versus localization of a light pulse by a subwavelength metal slit Phys. Rev. B 70, 195428-1-195428-9 (2004).
- [26] Petersson L. E. R. and Smith G. S. Transmission of an inhomogeneous plane wave through an electrically small aperture in a perfectly conducting plane screen J. Optical Soc. Amer. A. 21 975-980 (2004).
- [27] Degiron A., Lezec H. J., Yamamoto N. and Ebbesen T. W. Optical transmission properties of a single subwavelength aperture in a real metal Opt. Commun. 239 61-66 (2004).
- [28] Yin L. et al. Surface Plasmon at sSingle Nanohole in Au Films Appl. Phys. Lett. 85 467-469 (2004).
- [29] Chang S. H. et al. Surface plasmon generation and light transmission by isolated nanoholes and arrays of nanoholes in thin metal films Opt. Express 13 3150-3165 (2005).
- [30] Popov E. et al. Surface plasmon excitation on a single subwavelength hole in a metallic sheet Appl. Opt. 44 2332-2337 (2005).
- [31] Garcia-Vidal F. J. et al. Transmission of Light Through a Single Rectangular Hole in a Real Metal Phys. Rev.B 74 153411-4 (2006).
- [32] Kulkhlevsky S. V., Mechler M., Samek O. and Janssens K. Analytical model of the enhanced light transmission through subwavelength metal slits: Green's function formalism versus Rayleigh's expansion, Appl. Phys. B: Lasers and Optics, 84, 19-24 (2006).
- [33] Kindler J., Banzer P., Quabis S., Peschel U. and Leuchs G. Waveguide properties of single subwavelength holes demonstrated with radially and azimuthally polarized light Appl. Phys. B, 89, 517-520 (2007).
- [34] Genet C. and Ebbesen T. Light in tiny holes Nature, 445, 39-46 (2007).
- [35] de Leon-Perez F., Brucoli G., Garcia-Vidal F. J. and Martin-Moreno L. Theory on the scattering of light and surface plasmon polaritons by arrays of holes and dimples in a metal film New J. Phys., 10, 105017 (2008).
- [36] Przybilla F. et al. Efficiency and finite size effects in enhanced transmission through subwavelength apertures Opt. Express 13 9571-9579 (2008).
- [37] Nikitin a. Y. et al. Surface Electromagnetic Field Radiated by a Subwavelength Hole in a Metal Film Appl. Phys. Lett. 105 073902-4 (2010).
- [38] Yi J. M. et al. Diffraction Regimes of single Holes Appl. Phys. Lett., 109 023901-5(2012).
- [39] Rotenberg N. et al. Plasmon Scattering from Single Subwavelength Holes Appl. Phys. Lett. 108 127402-5 (2012).
- [40] Raether H. Surface Plasmons on Smooth and Rough Surfaces and on Gratings Springer-Verlag, Berlin (1988).